Measurement Science and Technology

A new sensor for the micrometre-level measurement of three-dimensional, dynamic contours

To cite this article: Tony Schmitz and John Ziegert 1999 *Meas. Sci. Technol.* **10** 51

View the article online for updates and enhancements.

Related content

- Some performance characteristics of a multi-axis touch trigger probe
F M M Chan, E J Davis, T G King et al.
- Scanning tunneling microscopy-based in situ measurement of fast tool servo-assisted diamond turning micro-structures
Bing-Feng Ju, Wu-Le Zhu, Shunyao Yang et al.
- Accurate identification and compensation of geometric errors of 5-axis CNC machine tools using double ball bar
Ali Lasemi, Deyi Xue and Peihua Gu

Recent citations

- Design, Modelation and Numerical Simulation of a Novel Artefact for Coordinate Measuring Machines Calibration Based on Laser Trilateration
M. A. Facas Vicente
- Coordinate metrology uncertainty using parallel kinematic techniques
J. Suzanne Canning *et al*
- Vision-based kinematic calibration of an H4 parallel mechanism: practical accuracies

This content was downloaded from IP address 152.15.112.62 on 27/11/2017 at 16:59

Meas. Sci. Technol. **10** (1999) 51–62. Printed in the UK PII: S0957-0233(99)98028-1

A new sensor for the micrometre-level measurement of three-dimensional, dynamic contours

Tony Schmitz and John Ziegert

Machine Tool Research Center, Department of Mechanical Engineering,
University of Florida, Gainesville, FL 32611, USA

Received 10 October 1998, in final form and accepted for publication 16 November 1998

Abstract. In this research, the implementation of simultaneous trilateration to measure three-dimensional, dynamic computer-numerically controlled (CNC) contours using the laser ball bar was investigated. The motivation behind this work is the desire to perform rapid, pre-process verification of CNC part paths without machining a test part. This reduces scrap and increases process efficiency. A prototype simultaneous trilateration laser ball bar (STLBB) system was designed, constructed and tested. Verification testing of the STLBB system was also completed. This investigation was composed of two parts: (i) comparisons between dynamic, two-dimensional paths measured both with the STLBB system and with an optical grid encoder; and (ii) static and dynamic reproducibility evaluation. Good agreement between the STLBB system and independent measurement devices provided authentication of the STLBB measurement capabilities. Once the validity and reproducibility of the STLBB system as a dynamic measurement tool had been confirmed, several three-dimensional CNC contour measurements were performed at micrometre-level accuracy.

Keywords: spatial coordinates, linear displacement interferometer, laser ball bar, simultaneous trilateration, dynamic contouring accuracy

1. Introduction

Computer-numerically controlled (CNC) multiple-axis machine tools are an essential component of modern manufacturing. As the requirements for accuracy and process efficiency increase, so do the demands for rapid and precise measurements of the three-dimensional motions of the machine tools.

The topic of modelling and prediction of machine-tool accuracy is not new and many volumes of high-quality research have been published. Two prevalent methods for the capture of experimental data have been described in this past work; namely static and dynamic data collection. For the most part, national and international standards for the geometrical calibration of machine tools have adopted methods of static measurement (i.e., the machine axis is stopped at regular or random intervals, the machine dynamics are allowed to settle and then several measurements are taken to average out machine noise). Dynamic measurement techniques are more common in spindle analysis (e.g. the 'grease pencil test' for the measurement of axis-of-rotation errors [1]), although recent work has also investigated the adaptation of dynamic measurements to geometrical calibration [2, 3].

The focus of this work is on the design, construction and testing of a sensor (the simultaneous trilateration laser ball bar system) which can perform dynamic, three-dimensional measurements of CNC contours to micrometre accuracy. These measurements are performed at the tool point in an attempt to close the otherwise open-loop mode in which machine tools operate (i.e., although the positions of the individual axes are servo-controlled, the actual spatial coordinates of the tool or end effector are unknown). This method differs from the geometrical calibration of machine tools, which measures the individual errors along each machine axis (three translational, three angular) and the squareness error(s) between the axes. These errors (21 for a three-axis machine tool) are then used as the input to a kinematic model (composed of a series of homogeneous transformation matrices (HTMs)) which is used to predict the tool-point errors. A thorough discussion of HTMs and kinematic modelling of machine tools can be found in [4]. The reader is also referred to [10] for a rigorous description of the methodology used to predict the geometrical positioning performance of machine tools.

The pre-process measurement of actual multi-axis contours would permit rapid verification of CNC part programs without the necessity of machining a test part. This reduces scrap and increases the manufacturing process efficiency, especially in situations in which the duration of machining is high and material is expensive (e.g. the aerospace industry). The data obtained from the

 © 1999 IOP Publishing Ltd

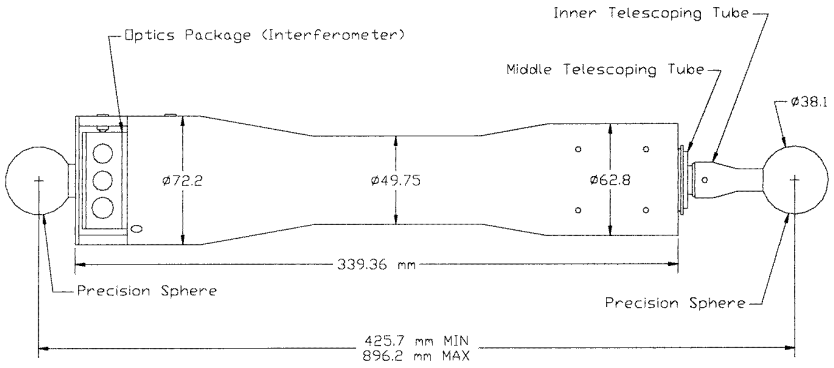

Figure 1. The laser ball bar.

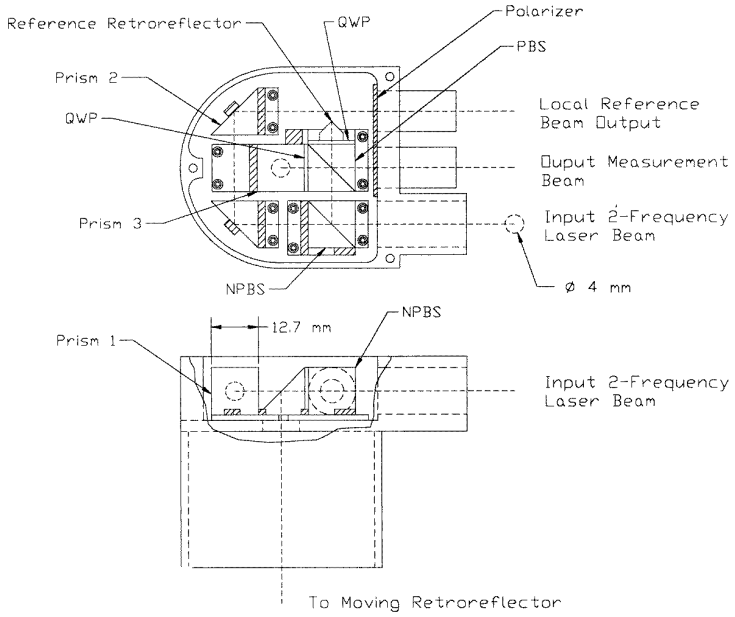

Figure 2. The LBB optics package.

3D measurements are also useful for the evaluation of the controller performance during contouring and the measurement of the relative contributions both of quasi-static positioning errors and of controller errors to the part dimensional errors.

2. A description of the sensor

The simultaneous trilateration laser ball bar (STLBB) system is based on the laser ball bar (LBB), a precision linear-displacement-measuring device developed at the University of Florida by Ziegert and Mize [5]. It consists of a two-stage telescoping tube with a precision sphere mounted at each end. See figure 1. A heterodyne displacement-measuring interferometer is aligned inside the tube and measures the relative displacement between the two sphere centres. The heterodyne signal (He–Ne, two-frequency laser light) is carried from a frequency-stabilized laser head to the Michelson-type interferometer by a single-mode, polarization-maintaining (SMPM) fibre. At the LBB, a local reference is generated in order to eliminate cable-induced phase shifts (e.g. mechanical or thermal deformations) in the SMPM fibre. The local reference and measurement signals are carried to the phase-measuring electronics (after passing through a polarizing filter oriented at 45° to the two orthogonal frequencies to provide interference) via two multi-mode (MM) optical fibres. The final linear displacement is calculated by taking the difference of the measurement and local reference signals. The LBB has been shown to be accurate to sub-micrometre levels during static measurements [6].

Figure 2 displays the optics package located in each LBB. The 4 mm diameter input laser beam is shown on the lower right-hand side of the top view. This beam is split into two components by the non-polarization beam splitter (NPBS). The transmitted portion (approximately 15%) is routed around the set-up (via prisms 1 and 2) through a polarizing filter oriented at 45° to the two orthogonal polarizations in the heterodyne signal. The two frequency components then interfere at the polarizing filter. The interference signal is carried by a MM fibre to a photodetector, where the electronic local reference signal is generated. The portion reflected from the NPBS travels to the Michelson

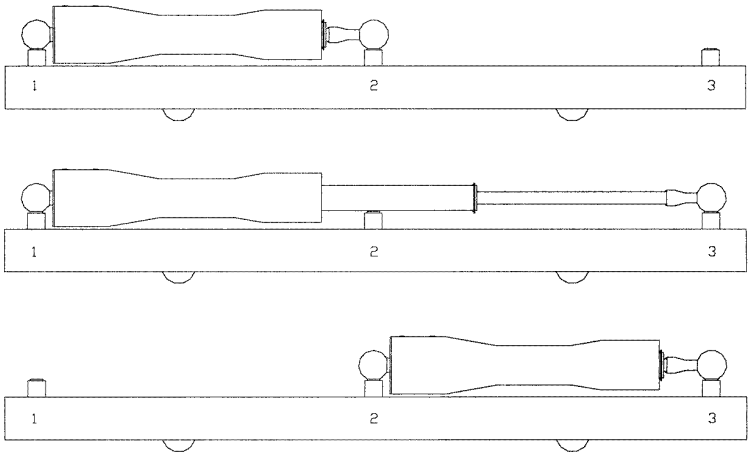

Figure 3. The LBB initialization procedure.

interferometer. At the polarization beam splitter (PBS), the vertical, 's', polarization is reflected and the horizontal, 'p', polarization is transmitted. The linearly polarized 'p' light then passes through a quarter-wave plate (QWP), orientated at 45° to the 'p' polarization, which converts the polarization state to circular. After three internal reflections within the retroreflector, the light returns parallel (and coaxial) to itself and passes once again through the QWP. The circular polarization state is now transformed into a linear one, but now the polarization vector is rotated by 90° with respect to the original orientation (a 180° relative phase shift between the electrical and magnetic fields has occurred). The light returning from the reference retroreflector is therefore functionally 's' light and is reflected at the PBS.

The 's' light originally reflected by the PBS follows an analogous path, except for the 90° turn imposed by total internal reflection in prism 3 (attached to the corresponding QWP). When the two light beams (with some relative Doppler phase shift) recombine at the PBS and pass through the polarizing filter (oriented at 45° to either linear polarization), they also interfere and are carried to the measurement photodetector (again on a MM fibre). Any phase change in the local reference signal is then subtracted from the measurement signal by the system electronics in order to obtain the final measurement signal, which represents the actual retroreflector motion.

Because the linear-displacement interferometer is able to measure changes only in displacement, not in absolute distance, each LBB must be initialized in order to determine the sphere-centre-to-sphere-centre length prior to use. The initialization procedure is composed of three steps. First, the LBB is placed between sockets 1 and 2 of the initialization fixture and the displacement counter zeroed. Next, the LBB is extended from socket 2 to socket 3 and the displacement recorded. This displacement is the distance between sockets 2 and 3. Finally, the LBB is placed between sockets 2 and 3 and the length of the LBB initialized to the previously recorded displacement. See figure 3. The entire procedure takes approximately 1 min, so any length changes in the initialization fixture due to thermal fluctuations are minimized.

Once it has been initialized, the LBB uses trilateration to measure the spatial coordinates of points along a CNC part path. The six edges of a tetrahedron formed by three base sockets (rigidly attached to the machine table) and a tool socket (mounted in the spindle) are measured and, by geometry, the spatial coordinates of the tool position in the LBB coordinate system are calculated. The three lengths between the three base sockets (L_{B1}, L_{B2} and L_{B3}) shown in figure 4 are measured once and remain fixed during the motion of the tool socket. These lengths are measured by extending the LBB between two adjacent base sockets and recording the LBB length (for example, L_{B1} is the length measured between base sockets 1 and 2). Because the base sockets are fixed to the machine table, it suffices to measure the three base lengths once (typically prior to the measurement of the three base-to-tool socket lengths).

The three base-to-tool socket lengths (denoted L_1, L_2 and L_3 in figure 4) are measured during execution of the applicable CNC part program. Once the coordinates in the LBB frame have been determined, they may be transformed into machine coordinates using the HTM between the LBB and machine coordinate systems. This HTM is obtained through an independent measurement using the STLBB system. (See appendix A.) Of particular interest is the fact that the measurement procedure requires no tedious alignment with the machine-tool axes of motion. The only requirement for the base-socket placement and numerically controlled contour programming is that no measurement point may lie outside the STLBB system work volume.

Previous research using the LBB has focused on sequential trilateration and quasi-static measurements (i.e., motion is stopped to perform the base-to-tool socket-length measurements) [7, 8]. In sequential trilateration, the same part path is traversed three times, measuring the lengths of one base-to-tool socket leg at a number of static points during each repetition. The set-up for sequential trilateration is shown in figure 5. This method requires a spatially reproducible measurement trigger since the tool socket must be in exactly the same position (for a given point) for each of the three measurements. When quasi-static measurements are performed, the machine reproducibility governs the accuracy of the measurement trigger and, therefore, the measured

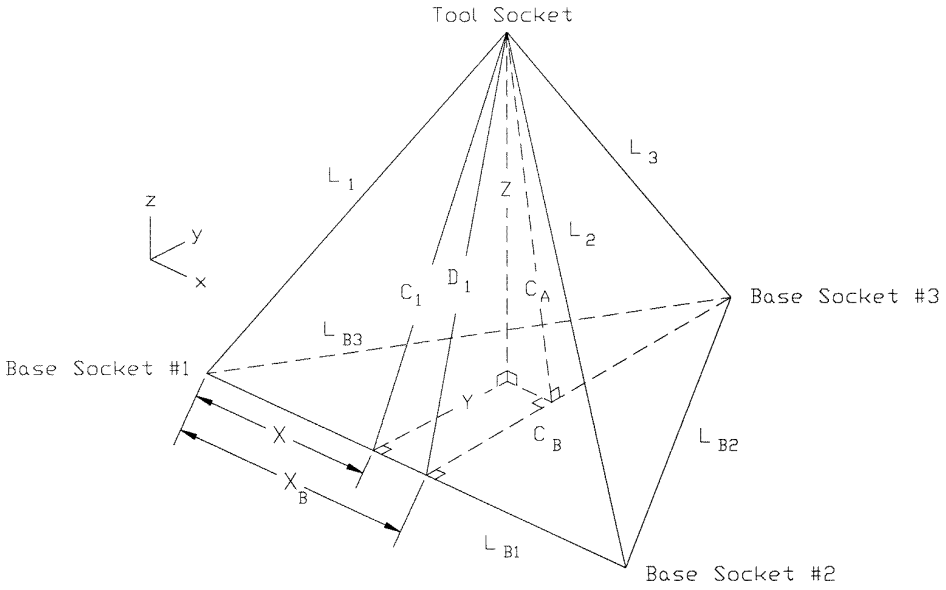

Figure 4. The trilateration tetrahedron.

coordinates. For most machine tools, the short-term static reproducibility is substantially better than the absolute positioning accuracy and this process yields satisfactory results. However, for dynamic path measurements, it is difficult to implement a spatially reproducible measurement trigger.

This research focuses on simultaneous trilateration, whereby three LBBs ride on a single precision sphere at the tool point to completely define all three base-to-tool socket lengths with one execution of the CNC program. Since all three leg lengths are captured at once, the measurement trigger need not be spatially reproducible and this method is better suited to dynamic measurements. See figure 6. In previous work, the feasibility of using the LBB as a dynamic measuring device was demonstrated [9]. Sequential trilateration was implemented to measure the coordinates of a dynamic 2D circular contour using one LBB and the encoder feedback signal as a measurement trigger. Measurements obtained using an independent device verified the LBB results.

Figure 7 shows a closer view of the spherical joint (located at the tool socket) which supports the three LBBs during simultaneous trilateration. Simultaneous trilateration requires that the axes of the three LBBs meet at a single point which coincides with the tool point (to minimize Abbé offset errors). During the execution of a CNC part program, the coordinates of the tool point are measured at closely spaced intervals along the path to define the contouring accuracy. Because the spatial coordinates of the tool point vary, both the lengths of the individual LBBs and the angles between the LBBs change. This calls for a joint which provides three independent angular degrees of freedom while prohibiting relative translations between the end points of each of the three LBB axes (e.g. a spherical joint).

For this research, the tool socket joint was attached to the machine spindle at a typical tool offset by a stiff bracket (approximately 1 μm deflection under maximum loads) mounted on a standard tool holder. The spindle was then locked against possible rotation during the measurements. One of the LBBs was attached to the grade 5, 38.1 mm diameter tool sphere by a removable threaded stud and three-point contact, while the other two were held in place by neodymium magnets mounted in three-point contact sockets. The three-point kinematic mounts were necessary to ensure that the location of the intersection of the three LBB axes (ideally at the sphere geometrical centre) did not change as the angular orientation of the LBBs varied during path motion.

During initial dynamic testing, it was observed that, under high accelerations, the two LBBs attached with the neodymium magnets tended to tip off the sphere rather than slide around it due to there being insufficient attractive force. The maximum magnet size was constrained by interference between adjacent LBBs during motion. Therefore, the spring aid assembly was implemented. This device applied an axial force through the approximate sphere centre while providing the necessary (spherical) degrees of freedom.

3. The verification of the sensor

The first step in the verification of this sensor was to compare the STLBB results with those of an independent sensor under the same measurement conditions. Ideally, a verification device which could measure the same 3D dynamic contours as the STLBB system would be selected. However, the closest match to this 3D dynamic requirement was provided by an optical grid encoder, which is capable of 2D dynamic measurements. The grid encoder used in this research was provided by the Heidenhain Corporation.

The Heidenhain KGM 101 grid encoder is composed of a grid plate (140 mm diameter) with a waffle-type grating of closely spaced lines (4 μm signal period) and a non-contact scanning head which is able to measure translations in two directions. The optical grid plate is attached to an aluminium mounting base. This base is mounted in the plane to be

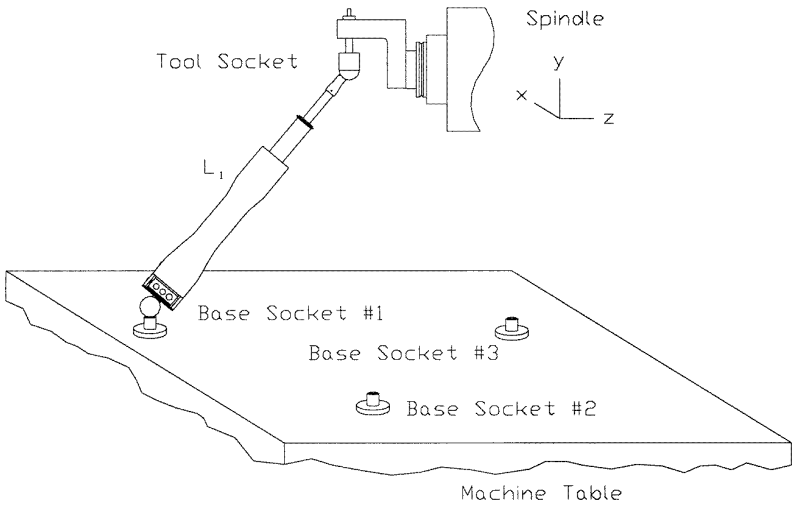

Figure 5. Sequential trilateration.

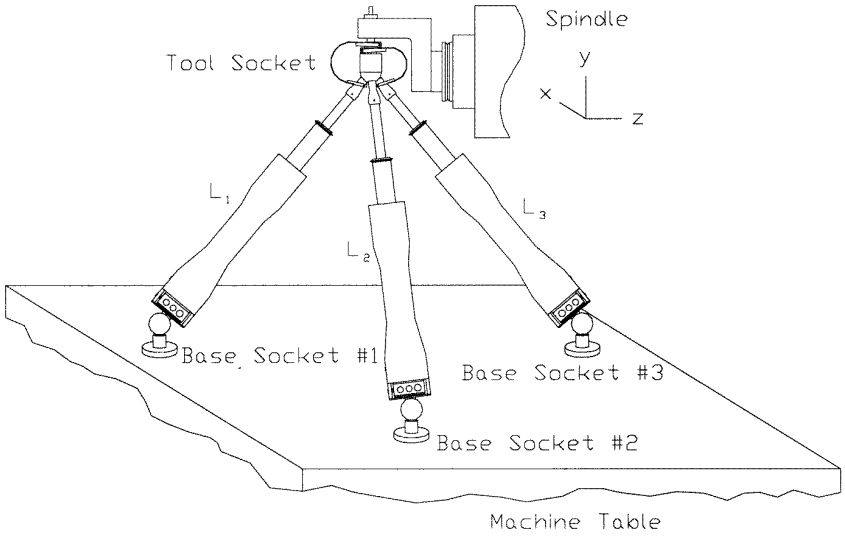

Figure 6. Simultaneous trilateration.

measured (on an X–Y table for instance) and the scanning head is fixed perpendicular to the plate (e.g. on the Z axis attached to the spindle). This system measures the relative planar motion of the two bodies for any curvilinear path in the plane of the mounting base with a resolution of 4 nm and to within an accuracy of ± 2 μm. The recorded motions allow the user to observe the dynamic effects of the machine tool's performance on 2D CNC tool paths. Figure 8 shows the Heidenhain set-up used for the 2D measurements. The STLBB system set-up for the verification measurements can be seen in figure 6. Note that the measurement point is on the spindle centreline with the same Z direction offset for both experimental set-ups. Therefore, geometrical error variations within the work volume will not introduce a relative difference (due to an Abbé offset) between the measurements. Additionally, the CNC programs both for the STLBB tests and for the Heidenhain tests were executed from the same starting coordinates so, again, any geometrical variations within the machine tool's work volume would be minimized. Finally, the part programs were run in the same order from a cold machine state to minimize thermal deviations between the two sets of tests.

Several planar contours were selected to be measured both with the Heidenhain grid encoder and with the STLBB system. These contours and the pertinent dimensions are summarized in figure 9. The data gathered from the Heidenhain measurements were adequate to fully verify the STLBB measurements on the basis of the following three-point argument. First, the STLBB system requires no special alignment of its axes with the machine tool's coordinate system and, in general, they are not aligned. Second, although the commanded path is in two dimensions with respect to the machine tool, the spatial coordinates of this path lie in three dimensions in the STLBB system. (The positions in the machine's coordinate system are then transformed using a rotation matrix obtained by an independent LBB measurement to give the final 2D results in machine coordinates.) Third, a typical contour will require extension or contraction of all three individual LBBs, a rotation of the LBBs within their respective sockets (a change

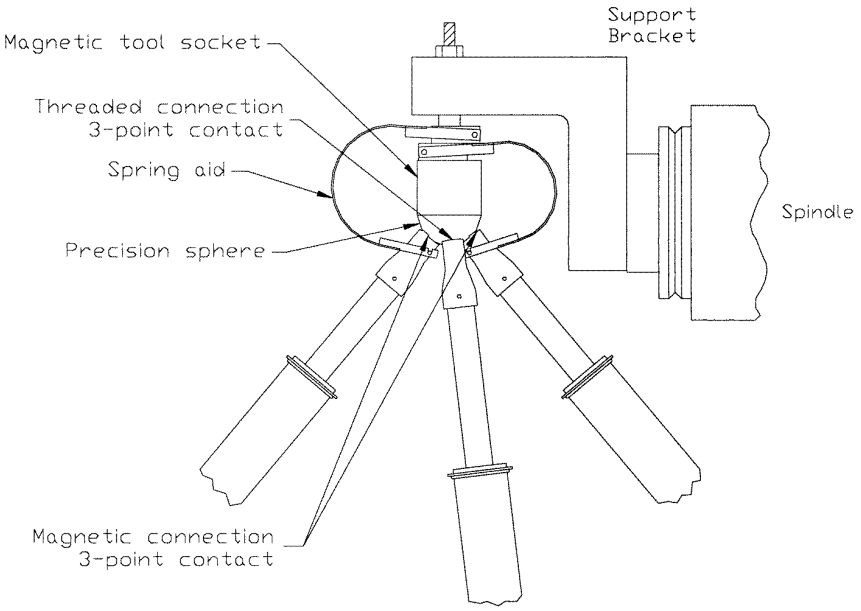

Figure 7. The tool-socket joint.

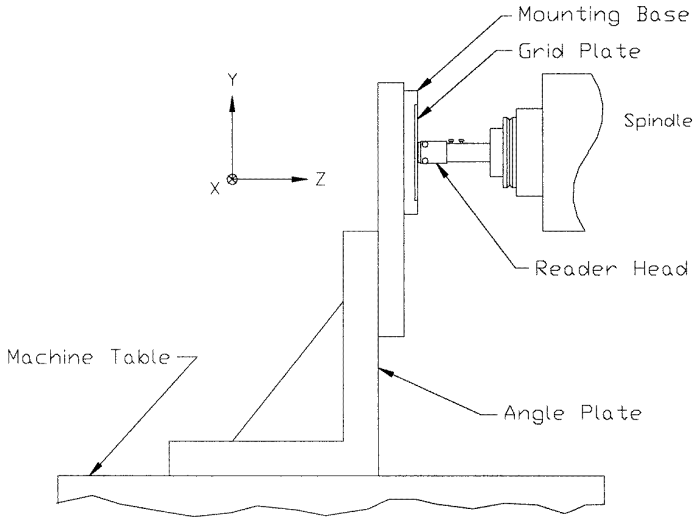

Figure 8. The Heidenhain grid-plate set-up.

in angular orientation) or both. Therefore, even though the commanded path lies in two dimensions in a coordinate frame external to the STLBB system, the path experienced by the STLBB system and the required motions of the individual LBBs are three dimensional in nature.

Comparisons between the Heidenhain and STLBB measurements will now be presented. Each of the six verification contours (angle, step, sultan, square, triangle and circle) will be discussed separately in the following paragraphs. All paths were executed at constant accelerations (i.e. trapezoidal velocity profiles) of 0.98–4.91 m s^{-2} with feed rates in the range 889–1778 mm min^{-1} (35–70 inches min^{-1}). Additionally, a small motion in the positive X and Y directions was commanded prior to the execution of each CNC contour in order to minimize the effects of possible reversal errors in each axis and a nominal temporal sampling frequency of 1 kHz was employed.

3.1. The angle path

The angle path includes motions in the X–Y plane which require linear interpolation in the two axes simultaneously. Figure 10 shows a comparison between the Heidenhain grid plate and STLBB measurements for a feed rate of 889 mm min^{-1} and an acceleration of 0.98 m s^{-2}. Only the cornering portion of the path is shown, in order to enhance the viewing resolution. Figure 11 exhibits the two measurements for a feed rate of 1778 mm min^{-1} and an acceleration of 4.91 m s^{-2}.

This path aids in the tuning of the servomotors on machine tools. The measured response (e.g. an undershoot or overshoot) can be used to set the individual axis gains. For the machine tool used in this research, a difference in the gain between the X and Y axes caused a steady-state positional error. Therefore, the actual contour is spatially

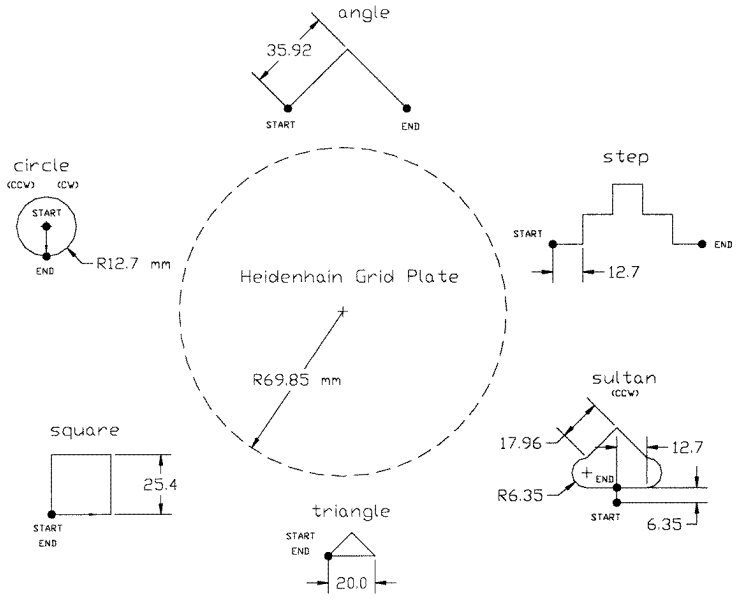

Figure 9. STLBB verification contours.

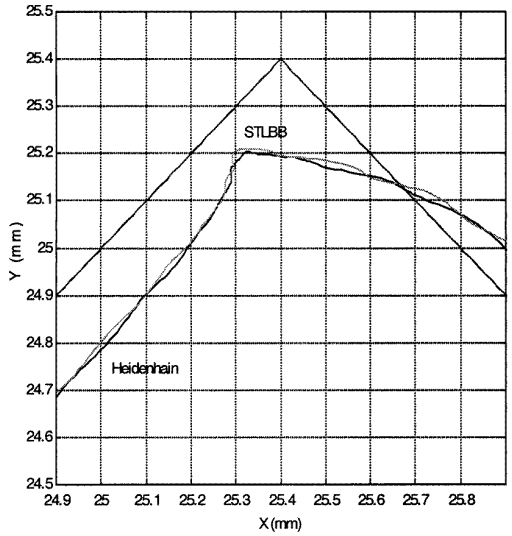

Figure 10. An angle-path comparison (889 mm min^{-1}, 0.98 m s^{-2}).

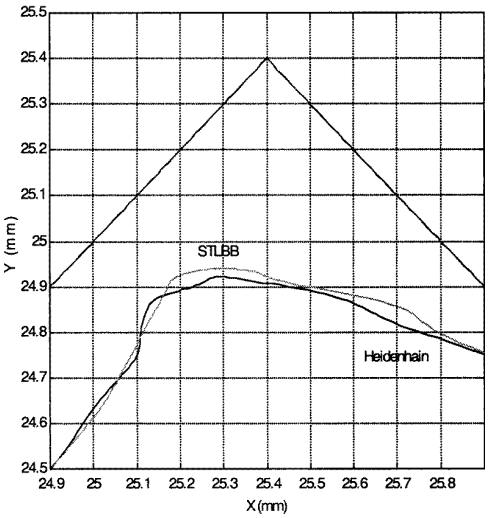

Figure 11. An angle-path comparison (1778 mm min^{-1}, 4.91 m s^{-2}).

offset from the commanded contour during constant-velocity motion. Because this error is proportional to the commanded feed rate, the offset in figure 11 is seen to be larger than that in figure 10.

3.2. The step path

The step path includes linear interpolation in the X and Y axes individually and sharp corners with both positive and negative Y direction motions. Consequently, this path can also be used to set the axes' gains during tuning. Figure 12 shows a comparison between the Heidenhain and STLBB measurements for the first cornering motion ($+X$ to $+Y$) in the path at a feed rate of 1778 mm min^{-1} and an acceleration of 0.98 m s^{-2}. Figure 13 displays the same contour section at a feed rate of 1778 mm min^{-1} and 4.91 m s^{-2} acceleration.

3.3. The sultan path

The sultan path combines simultaneous X–Y linear interpolation with circular interpolation and single-axis linear interpolation. This path integrates the angle and step tests with circular interpolation and gives a good overall picture of the machine's contouring performance. A small section of the measured path has been highlighted in figures 14 and 15. This section corresponds to the first transition from circular to linear interpolation in the contour (i.e. the right-hand side of the path directly above the counter-clockwise circular section). Figure 14 displays the measurement comparison for 889 mm min^{-1} feed rate. Figure 15 shows the contour section for 1778 mm min^{-1} feed rate.

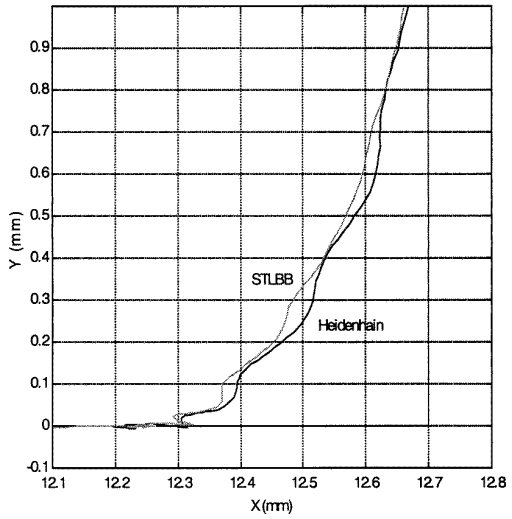

Figure 12. A step-path comparison (1778 mm min^{-1}, 0.98 m s^{-2}).

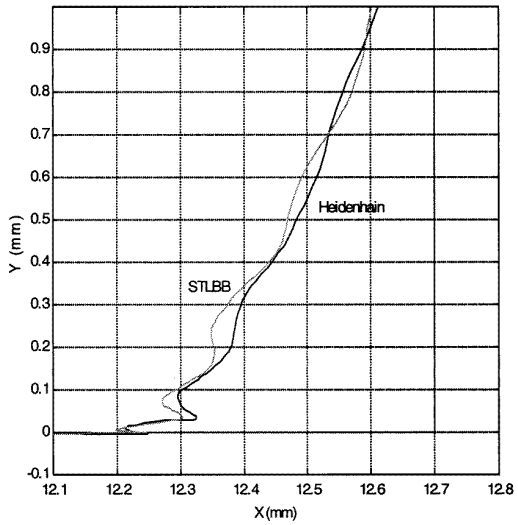

Figure 13. A step-path comparison (1778 mm min^{-1}, 4.91 m s^{-2}).

3.4. The square path

The square path provides linear interpolation in the X and Y coordinate directions as well as motions both in the positive and in the negative directions. It also provides a closed-loop path which can be used to evaluate possible reversal errors. Therefore, the under/overshoot in cornering, as well as X and Y reversal errors, may be seen with this path. The results for a 1778 mm min^{-1}, 4.91 m s^{-2} contour are shown in figure 16. The displayed section is the upper right-hand corner of the counter-clockwise square (i.e. the transition from $+Y$ to $-X$ motion).

3.5. The triangle path

The triangle path is similar to the angle contour, but also provides a closed-loop path and negative X direction motion. Figure 17 shows a comparison between the Heidenhain and STLBB results for the lower right-hand portion of a path executed at 1778 mm min^{-1} and 1.96 m s^{-2}. This contour

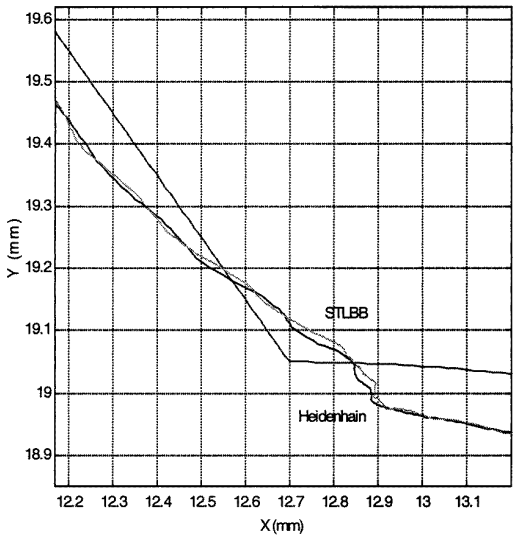

Figure 14. A sultan-path comparison (889 mm min^{-1}, 0.98 m s^{-2}).

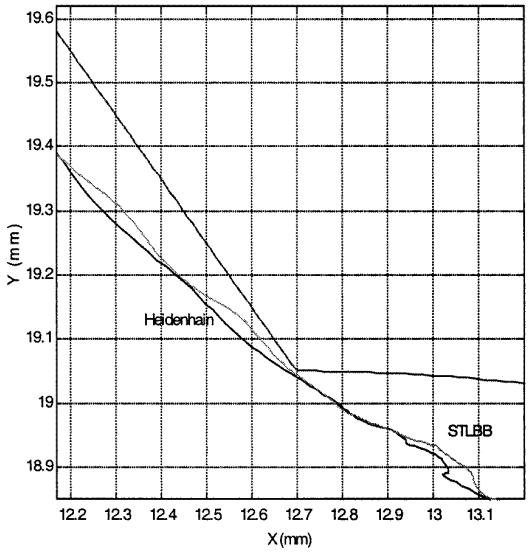

Figure 15. A sultan-path comparison (1778 mm min^{-1}, 0.98 m s^{-2}).

section represents the X motion reversal of the counter-clockwise triangle.

3.6. The circle path

A counter-clockwise circular path was also measured using the two measurement systems. Figure 18 displays the measurement results for a velocity of 1778 mm min^{-1}, with the radial deviations of the measured path from the commanded one amplified by a factor of five. Figure 18 shows that there is an elliptical distortion of the path with the major axis of the ellipse rotated 45° counter-clockwise from the positive Y axis. In this case, this elliptical distortion of the circular path was caused by the previously mentioned gain mismatch between the X and Y axes.

The good agreement between the optical grid plate and STLBB results for all feed rates and accelerations served to

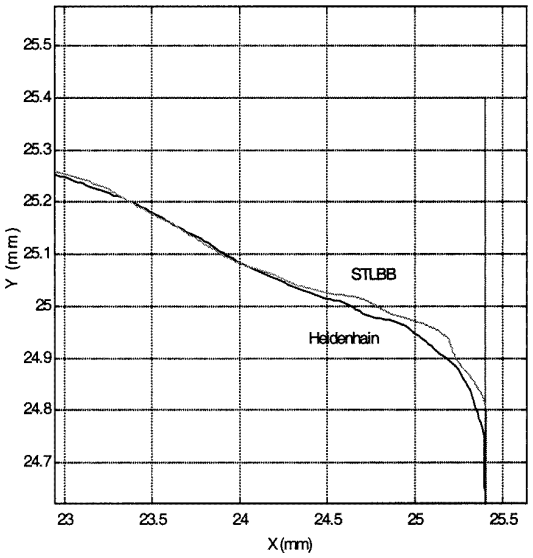

Figure 16. A square-path comparison (1778 mm min^{-1}, 4.91 m s^{-2}).

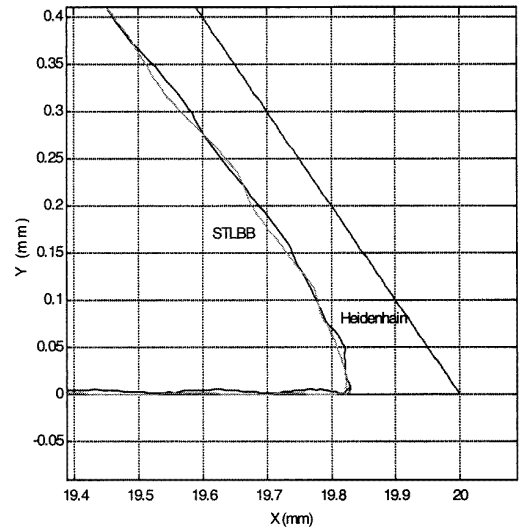

Figure 17. A triangle-path comparison (889 mm min^{-1}, 0.98 m s^{-2}).

verify the usefulness of the STLBB as a dynamic measuring device. In order to fully verify the STLBB system, both static and dynamic reproducibility tests were also completed. Static positioning tests were performed and the results compared with those obtained using a capacitance probe. In these tests, a short single-axis translation (i.e. a motion of 6.35 mm in the $+Y$ direction followed by a return to the starting position) was commanded and the start and end points recorded using both the STLBB and a capacitance probe. Sub-micrometre-level agreement between the two results was established.

To test the dynamic reproducibility, several back-to-back contours were measured both with the Heidenhain grid plate and with the STLBB system. In both cases, it was seen that consecutive measured paths fitted approximately within a 15 μm error band. However, it was also seen that the start/end points of the path were reproducible to sub-micrometre

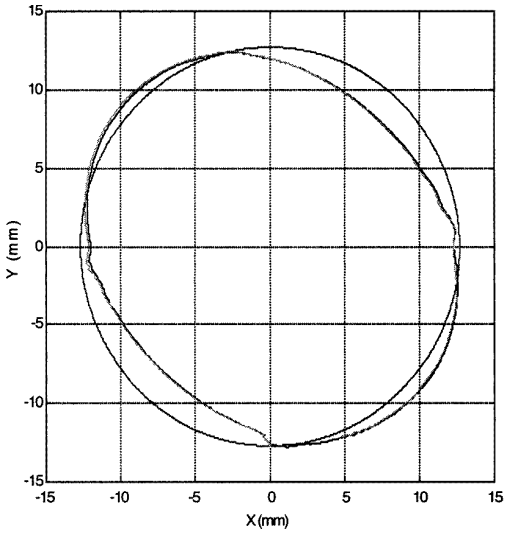

Figure 18. A circular-path comparison (1778 mm min^{-1}, 4.91 m s^{-2}).

accuracy. It was only during the dynamic sections of the contours that a relative difference was observed. Because the grid plate is a non-contact measuring device and does not affect the machine-tool dynamics, it was determined that the machine-tool controller was responsible for this path-dynamic non-reproducibility, rather than either of the measurement systems.

4. Three-dimensional contour measurements

Four different paths, which combine both linear and circular interpolation, were chosen to investigate the STLBB 3D measurement performance. The first path, shown with an STLBB measurement in figure 19, is corkscrew in nature. In figure 19 (as well as figures 20–25), the commanded path is represented by a broken line, while the actual contour measurement is displayed as a full line. For the corkscrew path, a counter-clockwise half circle was commanded in the X–Y plane, then a small step in the $-Z$ direction was executed. Next, the half circle was completed and followed by another step in the $-Z$ direction, etc. The second CNC program roughly simulated a hemispherical cutting path. First, a small circle was executed in the X–Y plane. Next, a step both in the $-Z$ and in the $-Y$ directions was commanded. A larger circle with the same centre coordinates was next executed from this new starting point. The completion of this circle was followed by another Y–Z linear step and so on. This path and a corresponding STLBB measurement are shown in figure 20. The final two paths were executed in a plane oblique to each of the machine tool's coordinate axes. Both a square and a circular path were commanded in order to investigate the effect of three simultaneous coordinate motions on path errors. These oblique plane contours, together with their respective STLBB measurements, are shown in figures 21 and 22.

Comparisons between the STLBB measurements and the commanded 3D paths are best made by viewing small sections of the individual contours. In figure 23, the transition from the first half circle to the first $-Z$ motion in the

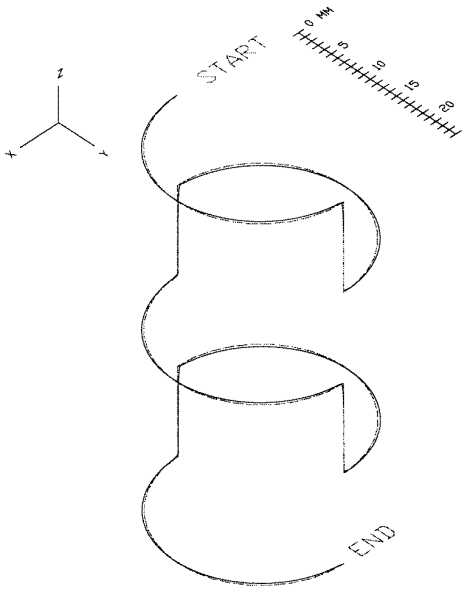

Figure 19. The STLBB corkscrew 3C path and STLBB measurement.

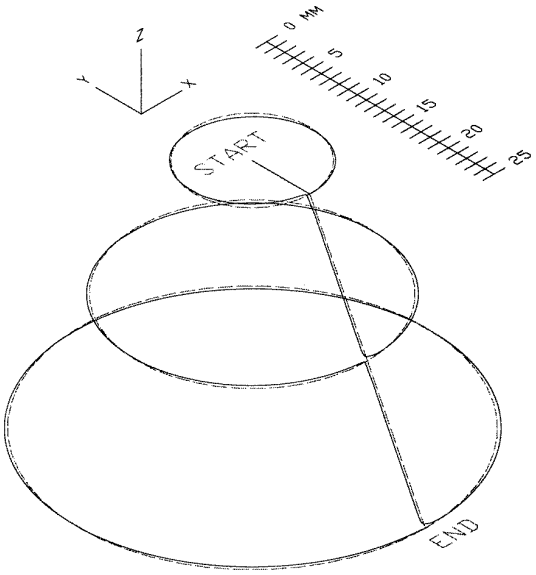

Figure 20. The STLBB hemisphere 3C path and STLBB measurement.

corkscrew path is shown. The elliptical distortion of the half circle in the X–Y plane is evident, as are the undershoots both in the X and in the Y directions for the start of the $-Z$ motion. The integral gain in the controller then begins to correct the steady-state error in the X and Y directions as the Z motion progresses.

Figure 24 shows the start and end points for the smallest circle in the hemispherical 3D path. It is immediately apparent that the circular path does not close and also exhibits the elliptical distortion due to the unequal X–Y controller gains. An X axis reversal error can also be seen as the short Y direction straight-line motion during the circular interpolation. It can also be recognized that the contouring accuracy in the transition from circular to linear interpolation is quite poor.

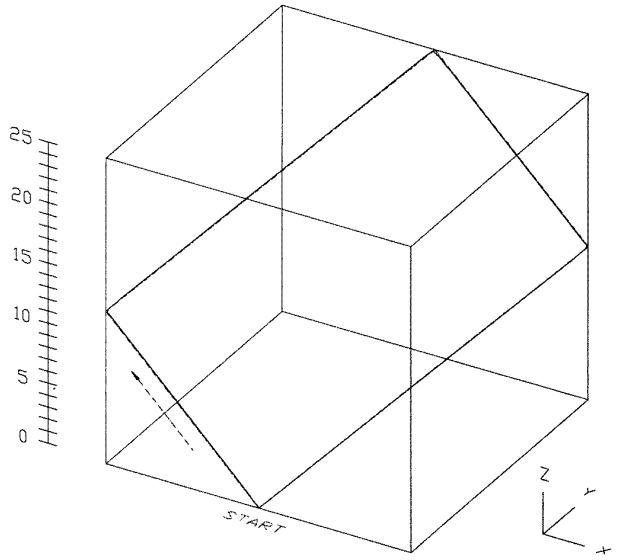

Figure 21. The STLBB oblique-square 3D path.

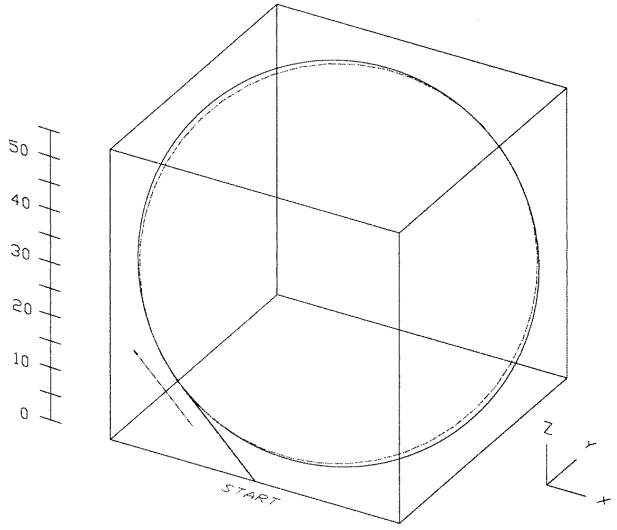

Figure 22. The STLBB oblique circular 3D path.

Figure 25 displays a comparison between two oblique rectangular paths executed at different feed rates (889 and 1778 mm min^{-1}). The section shown is the transition from $-X$, $+Z$ linear interpolation to $+X$, $+Y$, $+Z$ linear interpolation. Figure 25 shows that there are a steady-state error in the X–Z plane and undershoot errors at the interpolation direction transition. The individual X–Y, Y–Z and X–Z planes of motion for the 3D path section shown in figure 25 are given in figures 26–28. These plane views emphasize both the existence of errors in each of the coordinate directions for this path and the dramatic effect of the feed rate on the magnitude of these contouring errors.

5. Conclusions

In this research the implementation of simultaneous trilateration to measure three-dimensional CNC contours

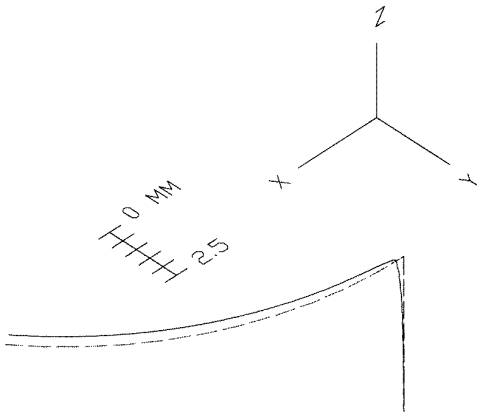

Figure 23. The STLBB corkscrew 3D path section.

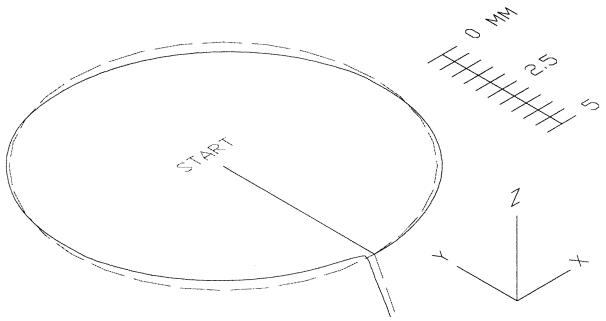

Figure 24. The STLBB hemisphere 3C path section.

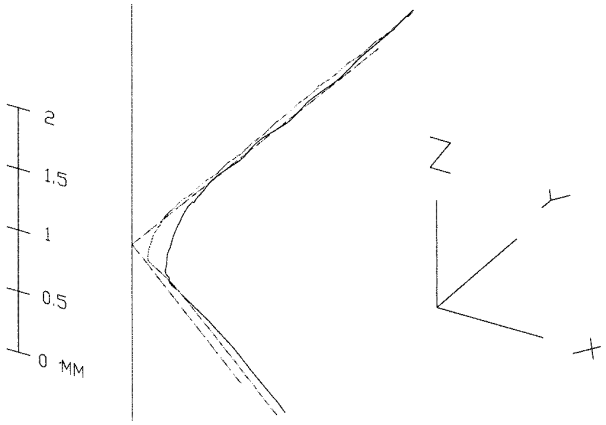

Figure 25. The STLBB oblique-rectangle 3D path section.

using the laser ball bar was completed. A prototype simultaneous trilateration laser ball bar (STLBB) system was designed, constructed and tested. The verification testing of the STLBB system was composed of two main parts. In the first set of tests, six two-dimensional contours were measured both with the STLBB system and with a Hiedenhain KGM 101 grid encoder. Both the path velocity and the acceleration were varied in order to study the corresponding effects. Good agreement between the STLBB and Heidenhain results at all velocities and accelerations provided authentication of the STLBB measurement capabilities.

The second group of verification tests included an evaluation of the static and dynamic measurement

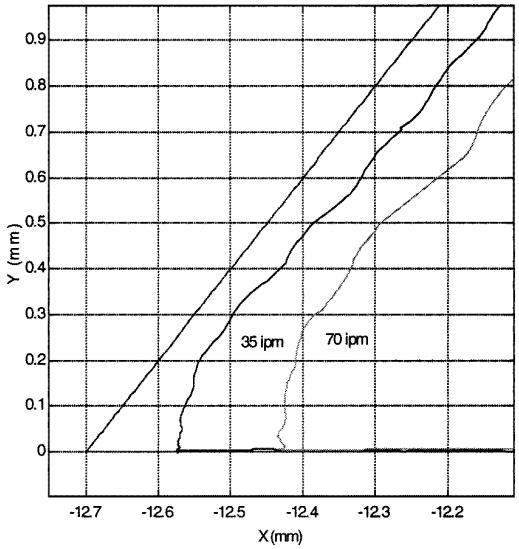

Figure 26. The STLBB oblique-rectangle X–Y plane.

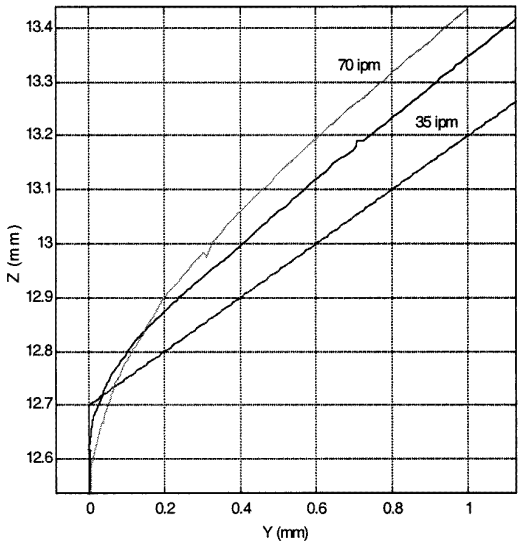

Figure 27. The STLBB oblique-rectangle Y–Z plane.

reproducibilities of the STLBB system. The static positioning reproducibility was tested by comparing the STLBB measurement results for a short, single-axis translation with capacitance-probe measurements of the same path. Sub-micrometre agreement between the return positioning errors recorded by the two methods was found.

The dynamic positioning reproducibility was evaluated using the Heidenhain grid encoder. In these tests, several back-to-back CNC paths were executed and the results recorded using both the STLBB and the Heidenhain measurement systems. For this particular machining centre, it was found that the dynamic positioning non-reproducibility of the machine tool was much larger than the measurement systems' resolutions. Using both systems, approximately a 15 μm error band was needed in order to enclose successive repetitions of an example NC path during dynamic motions, although the starting and ending points of the path were reproducible to sub-micrometre levels.

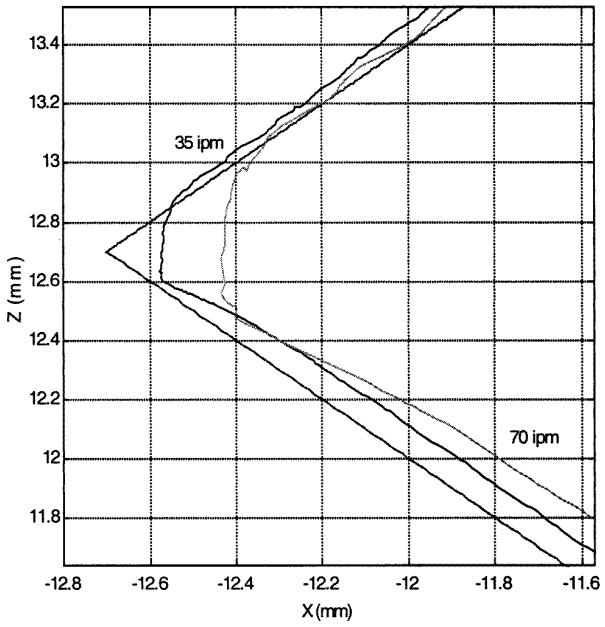

Figure 28. The STLBB oblique-rectangle X–Z plane.

Once the validity and reproducibility of the STLBB system as a dynamic measurement tool had been confirmed, the next step was to perform the inaugural measurement of three-dimensional CNC contours to micrometre-level accuracy. Four contours were selected to highlight the STLBB system's 3D measurement capabilities: a corkscrew, a hemisphere, an oblique-plane rectangle and an oblique-plane circle. These paths combined linear and circular interpolation in three simultaneous axes of motion. The measurement results revealed a large dependence of the path-contouring accuracy on the commanded feed rate, as well as the overall poor contouring performance (i.e. the measured path differed from the commanded one) for the three-axis machine tool used in this study.

Although the STLBB system is not the only sensor capable of three-dimensional, dynamic measurements (e.g. laser tracking interferometers also have this capability and, in general, have a larger work volume than that of the STLBB system), the STLBB system's accuracy level (of the order of ± 1 μm) and brief set-up time make it ideally suited to the measurement of dynamic, CNC contours on industrial machine tools.

Appendix A: transformation of laser ball bar coordinates into machine coordinates

A method to transform coordinates from the LBB frame {B} into a given machine frame {M} is outlined here [8]. The first step is to define a reference axis in the machine frame. In this approach, the reference axis is assumed to be the Z_M axis. The LBB is used to sequentially sample a set of points (x_i, y_i, z_i) at regular intervals along the positive Z_M axis. These coordinates are used to determine the best-fit line along this axis. The direction cosines of the best-fit line provide the components of the unit vector $\boldsymbol{n}_z$ in the LBB coordinates along the Z_M axis. Similarly, a set of points is sampled by moving along the X_M axis. Since the machine axes could have orthogonality (or squareness) errors between them, the direction cosines of the vector $\boldsymbol{V}_x$ derived from the X_M motion need not represent a unit vector orthogonal to the Z_M axis. However, a unit vector $\boldsymbol{n}_y$ which will lie in the Y_M direction can be defined by

$$\boldsymbol{n}_y = \frac{\boldsymbol{n}_z \times \boldsymbol{V}_x}{|\boldsymbol{n}_z \times \boldsymbol{V}_x|}. \tag{A1}$$

By evaluating $\boldsymbol{n}_y \times \boldsymbol{n}_z$, the unit vector $\boldsymbol{n}_x$ along the X_M axis is found. These unit vectors $\boldsymbol{n}_x$, $\boldsymbol{n}_y$ and $\boldsymbol{n}_z$ form a right-handed Cartesian coordinate system and represent the coordinate system of the machine as seen in LBB coordinates. The 3×3 rotation matrix for conversion between the ball-bar frame and the machine-tool frame can be expressed as

$$\mathbf{R}_B^M = \begin{bmatrix} \boldsymbol{n}_x \\ \boldsymbol{n}_y \\ \boldsymbol{n}_z \end{bmatrix}. \tag{A2}$$

The transformation between the two coordinate frames can then be expressed by the 4×4 matrix

$$\mathbf{T}_B^M = \begin{bmatrix} & \mathbf{R}_B^M & & \boldsymbol{D} \\ 0 & 0 & 0 & 1 \end{bmatrix}$$
$$\boldsymbol{D} = [D_x D_y D_z]^{\mathrm{T}} = [000]^{\mathrm{T}}. \tag{A3}$$

The final column, $\boldsymbol{D}$, in the transformation matrix defines the translation between the origins of the two coordinate frames. However, the $\boldsymbol{D}$ vector is set to zero in this method since all the machine errors are normalized with respect to the origin of the machine frame {M}.

References

[1] 1988 Draft revision of 'ASME/ANSI B89.3.4: dimensional metrology–axes of rotation standard, appendix D'
[2] Postlethwaite S, Ford D and Morton D 1995 Geometric errors from dynamic data–a novel calibration technique *Laser Metrol. Machine Performance* **2** 139–48
[3] Postlethwaite S, Ford D and Morton D 1997 Dynamic calibration of CNC machine tools *Int. J. Machine Tools Manufacturing* **37** 287–94
[4] Slocum A 1992 *Precision Machine Design* (Englewood Cliffs, NJ: Prentice-Hall)
[5] Ziegert J C and Mize C D 1994 Laser ball bar: a new instrument for machine tool metrology *Precision Engng: J. Am. Soc. Precision Engineers* **16** 259–67
[6] Mize C D, Ziegert J C, Pardue R and Zucker N 1994 Spatial measurement accuracy tests of the laser ball bar, final report for CRADA Y-1293-02244 between Martin Marietta Energy Systems and Tetra Precision, Inc
[7] Kulkarni R 1996 Design and evaluation of a technique to find the parametric errors of a numerically controlled machine tool using a laser ball bar *MS Thesis* University of Florida, Gainesville, FL
[8] Srinivasa N 1994 Modeling and prediction of thermally induced errors in machine tools using a laser ball bar and a neural network *PhD Dissertation* University of Florida, Gainesville, FL
[9] Schmitz T and Ziegert J 1998 Premachining CNC contour validation *Precision Engng: J. Am. Soc. Precision Engineers* **22** 10–18
[10] 1992 *Methods for Performance Evaluation of Computer Numerically Controlled Machining Centers* (New York: ASME)